

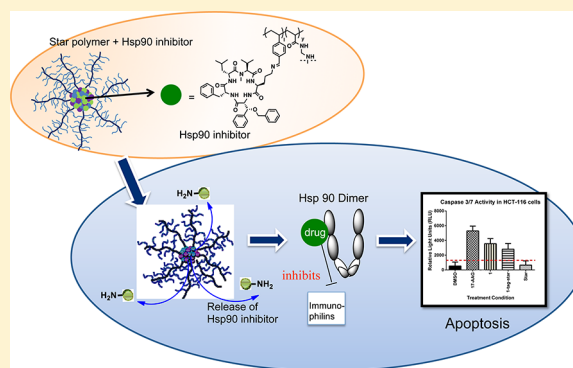
Effectively Delivering a Unique Hsp90 Inhibitor Using Star Polymers

Seong Jong Kim,[†] Deborah M. Ramsey,[†] Cyrille Boyer,[‡] Thomas P. Davis,[‡] and Shelli R. McAlpine^{*†}[†]Department of Chemistry, University of New South Wales, Sydney NSW 2052, Australia[‡]Australian Centre for Nanomedicine, University of New South Wales, Sydney NSW 2052, Australia

Supporting Information

ABSTRACT: We report the synthesis of a novel heat shock protein 90 (hsp90) inhibitor conjugated to a star polymer. Using reversible addition–fragmentation chain-transfer (RAFT) polymerization, we prepared star polymers comprising PEG attached to a predesigned functional core. The stars were cross-linked using disulfide linkers, and a tagged version of our hsp90 inhibitor was conjugated to the polymer core to generate nanoparticles (14 nm). Dynamic light scattering showed that the nanoparticles were stable in cell growth media for 5 days, and high-performance liquid chromatography (HPLC) analysis of compound-release at 3 different pH values showed that release was pH dependent. Cell cytotoxicity studies and confocal microscopy verify that our hsp90 inhibitor was delivered to cells using this nanoparticle delivery system. Further, delivery of our hsp90 inhibitor using star polymer induces apoptosis by a caspase 3-dependent pathway. These studies show that we can deliver our hsp90 inhibitor effectively using star polymers and induce apoptosis by the same pathway as the parent compound.

KEYWORDS: Heat shock protein 90, hsp90, macrocycles, cyclic peptides, nanoparticles, polymers, drug delivery, drug–peptide conjugation, star polymer



Heat shock proteins (hsps) are a family of essential molecular chaperones found in all cells, and expression levels of hsps are upregulated in the presence of environmental or toxicological stress.^{1–4} Ranging from 20 to 100 kDa in size, hsps maintain homeostasis and support cellular transport mechanisms.^{5,6} Hsps 90 and 70 are the most abundant hsps in normal or transformed cells, and hsp90 contributes 3–5% of the total protein load in tumors due to the metabolic demands required for rapid cell growth.^{4,7} Hsp90 assists cancer cell division and facilitates cell survival through interactions with over 200 proteins.^{8,9} Inhibition of hsp90 leads to destabilization of client proteins required for oncogenesis, which may explain why cancer cells exhibit a greater dependency on the heat shock response compared to normal cells.¹⁰ Fifteen inhibitors of hsp90 are being tested in 49 clinical trials.^{11–15} Although these leads are promising, all molecules under development share three major disadvantages: (a) they are structurally related to a single class of inhibitors, (b) they all target the same binding site, and (c) they all induce a heat shock response. Inducing the heat shock response presses four of the heat shock proteins into overdrive, which rescues the cells from death. This rescue effect is a significant problem in a cancer treatment. Thus, although hsp90 is a clinically viable target, there is a pressing need for new hsp90 inhibitors that overcome these limitations.¹²

Over the past 10 years, we have been working on the synthesis of hsp90 inhibitors^{16–} and have generated compound 1 (Figure 1) as a lead structure.²⁵ Compound 1 has demonstrated promise as a novel hsp90 inhibitor, and we

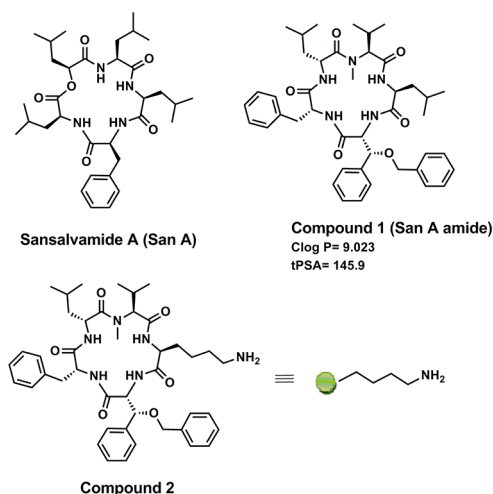


Figure 1. Sansalvamide A and compound 1 and 2.

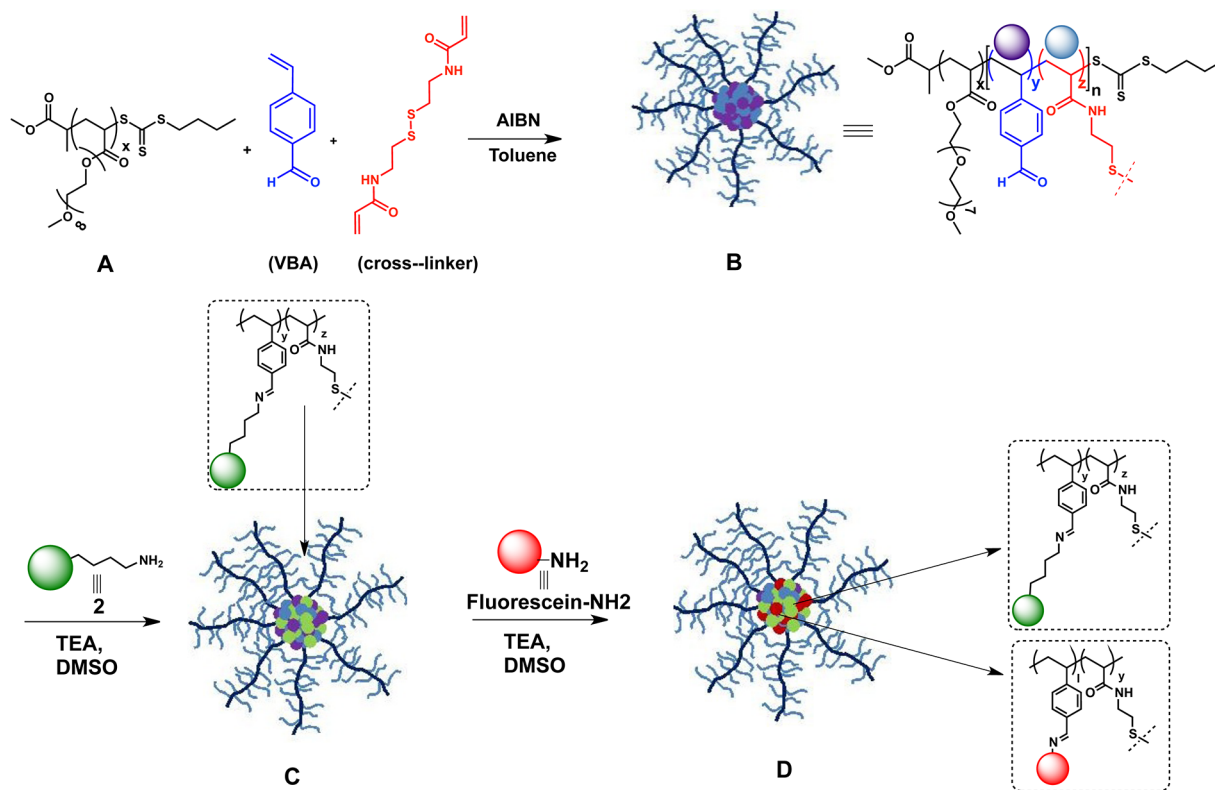
have published numerous papers proving that it targets this heat shock protein.^{19–22,24–25} It has several advantages over current hsp90 inhibitors including the following: our molecule selectively modulates a set of client proteins unique from those

Received: February 27, 2013

Accepted: July 25, 2013

Published: July 25, 2013

Scheme 1. Synthesis of Cross-Linked Star Polymer (A,B), Star Polymer Attached to Compound 2 (C), and Fluorescent Polymer (D)



regulated by current inhibitors,^{19,21} and it does not induce a heat shock response.^{19,21}

Compound 1 is cytotoxic against multiple cancer cell lines ($IC_{50} = 0.5\text{--}3\ \mu\text{M}$)²⁵ and binds to a unique site on hsp90, distinct from the ATP binding site that is targeted by all current clinical candidates. Although it modulates C-terminal client proteins and cochaperones, compound 1 does not bind to the same site as coumermycin or other C-terminal hsp90 inhibitors. Rather, compound 1 binds selectively to the N-middle domain of hsp90,^{19,21,22} controlling the binding between proteins that contain a tetratricopeptide (TPR) motif and the C-terminal MEEVD region of hsp90. Most significantly, compound 1 does not induce a heat shock response, unlike other hsp90 inhibitors.^{19,21,25} Thus, our compound shows tremendous potential as a preclinical candidate. Compound 1's ClogP value is 9.023, and improving its pharmacokinetic properties would involve increasing its solubility.²⁵ Compound 1 enters cells via a diffusion uptake mechanism; it is stable in cells and has an efflux ratio (B/A) of 3.²⁵ However, compound 1's poor solubility is its limiting factor for the next developmental stage.^{19,25}

Delivery of drugs using nanoparticles has been extremely successful for improving systemic circulation, water-solubility and drug protection, including the reduction of efflux mechanisms.^{26–29} Polymer conjugates have been approved by the FDA, with polyethylene glycol (PEG) being the most common choice for conjugation to small molecules.³⁰ Through building architecturally unique star polymers, we have produced highly water-soluble and biocompatible nanoparticles.^{31–34} Star polymers are structures where multiple several chains emanate from a single junction point known as the core, where this architecture has been verified.^{31–34} The core is held together

with a degradable disulfide linker, which can fall apart upon entering the cell. Since nanoparticles enter cells via endocytosis, in contrast to diffusion, they bypass Pgp efflux systems.³⁵

Herein, we report the synthesis of compound 2 conjugated to a star polymer (Scheme 1). Using RAFT polymerization, we prepared star polymers (B) comprising PEG attached to a pre-designed functional core with benzaldehyde and a disulfide cross-linker.³⁴ These star polymers were generated by using arm homopolymer (A), Vinyl benzaldehyde (VBA), and the cross-linker in a radical reaction to form (B). This process generated star polymers that were 14 nm in diameter, as determined by dynamic light scattering (DLS). This size is ideal for tumor penetration and accumulation.³⁶ The stars were cross-linked using disulfide linkages, generating nanoparticles that are easily degraded by the body (B).³⁴ Conjugating compound 2, which was our previously identified lysine version of compound 1 that bound to hsp90 (Scheme 1),²¹ to the star polymer generated star polymer C. We show via stability studies, growth inhibition assays, and confocal microscopy that compound 2 enters cells using this nanoparticle delivery particle C. In addition, we verify that entry of compound 2 leads to apoptosis by a caspase 3-dependent pathway, which is similar to the cell death mechanism induced by the parent compound (1).

We synthesized compound 2 via a solid phase strategy that we had previously reported.^{21,22} Compound 2 was reported as the optimized tagged version of compound 1.^{21,22} Indeed, we show that placement of the tag dramatically impacts the ability of compound 1 to bind to hsp90, and placement at the L-leucine position was optimal for binding and inhibiting the function of hsp90. Compound 2 was constructed with a preloaded 2-chlorotrityl (Clt) resin. Sequential coupling of

Table 1. Percent Growth Inhibition Values (GI%) of Compounds 1 and C in HCT-116 (Colon Cancer Cells)^a

	17AAG 100 μ M	1 5 μ M	B 10 μ M	C 1.16 μ M	C 3.33 μ M
GI %	34 \pm 1%	32 \pm 4%	0%	31 \pm 4%	64 \pm 4%

^aExperiments were performed in quadruplicate. The average growth inhibition values and the corresponding standard errors of the mean are reported for each treatment condition.

fluorenylmethyloxy carbonyl (Fmoc) protected amino acids and deprotection of the Fmoc group generated a linear pentapeptide.^{21,22} Cyclization was accomplished using a cocktail of four coupling agents (see Supporting Information), and benzylation of the hydroxy phenylalanine yielded the *tert*-butyloxycarbonyl (Boc)-protected lysine of compound 2. Boc-protected lysine was deprotected using 20% trifluoroacetic acid (TFA) in dichloromethane, and 2 was conjugated without purification.

The star polymer was constructed via a reversible addition–fragmentation chain-transfer polymerization (RAFT) method that was previously reported by the Davis group.^{21,22} Synthesis of the polymer arm A was performed using oligo(ethylene glycol) methyl ester acrylate (OEG- A_{480}). The poly(OEG) arm polymer ($M_n = 12\,000$ g/mol, PDI = 1.11) was chain extended in the presence of *N,N*-bis(acryloyl)cystamine as a cross-linker and VBA as a comonomer (Scheme 1) to generate star polymer B.¹⁸ Star polymer B thus contained PEG coronas and VBA (Scheme 1).³⁴ PEG coronas help polymer stabilization in biological media and contribute to antifouling,³⁷ stealth-like attributes,³⁸ and biocompatibility.³⁹ The star polymer properties are adjusted by manipulating the vinyl benzyl aldehyde composition in the cores. The star polymer and AIBN were reacted in a ratio of [polymer]/[cross-linker]/[VBA] = 1:8:6. The star polymer was purified by dialysis to remove all traces of unreacted monomers, cross-linker, or VBA. The star polymers were then purified by precipitation in diethyl ether.³⁴

The aldehyde functional group in VBA is conjugated to compound 2 via a pH-sensitive linkage (imine, Scheme 1).^{40,41} It is well-known that imine bonds are unstable in mildly acidic conditions and, specifically at pH = 5.5, within endosomes or lysosomes. Thus, conjugation at pH = 7 provides a stable linkage from which the molecule can be taken up via lysosomes, but upon sequestering the pH will drop to \sim 5.5, and the compound will be released in the cell.

We conjugated compound 2 and star polymer B in a 1:40 ratio (amine on peptide/aldehyde on polymer) with Et_3N (2 equiv) in DMSO (1 M) (Scheme 1).³⁴ These conditions led to imine formation and generated star polymer C. The unreacted compound 2 was separated from star polymer C using dialysis (MWCO = 3500 Da). DMSO was exchanged for water by membrane dialysis for 1 day (the solvent was changed every hour). The unreacted star polymer B was separated from star polymer C by HPLC. The structure and loading of star polymer C was confirmed using several different methods, including GPC ($M_n = 72\,000$ g/mol, PDI = 1.21), ^1H NMR spectroscopy, LC–MS, and UV–visible spectroscopy (Supporting Information).

DLS was used to determine the size and stability of the star polymer C that was dispersed in cell growth media (10% FBS in DMEM). DLS analysis confirmed an average nanoparticle size of \sim 14 nm, and the imine present in star polymer C was stable for 5 days (Figures S9 and S10, Supporting Information). These results verify that star polymer C remains stable in cell growth media during the time course required for biological assays.

Using standardized conditions,^{17,18,42} we measured cell proliferation of HCT-116 cells in the presence of 5 μ M of 1 or in the presence of two star polymer C concentrations. The respective concentrations of compound 2 that were delivered by star polymer C were 1.16 and 3.33 μ M, respectively (Table 1). Upon confirmation of purified star polymer C, we treated a colon cancer cell line (HCT-116) with this material and compared its potency to compound 1. It should be noted that directly treating cells with compound 2 without delivering it via polymer is noncytotoxic to HCT-116 cells.²⁵ Compound 2 has a protonated amine that inhibits passive diffusion through the cell membrane, making compound 1 the best positive control. Star polymer C, which contained the nanoparticle delivering 1.16 μ M of compound 2 (Table 1), inhibited cell proliferation to the same degree as 5 μ M of compound 1 alone, indicating that the star peptide improved the potency of compound 1 by 5-fold. Further, when star polymer C delivered 3.33 μ M of compound 2, the GI% showed a 2-fold increase in cytotoxicity over compound 1 alone ($P = 0.0001$). Note: star polymer B (nanoparticle without hsp90 inhibitor) is completely nontoxic (Figure S13, Supporting Information). These data show that the nanoparticle delivery vehicle coupled to compound 2 is more potent than 1 alone, and the improved potency must be due to better cellular uptake of star polymer C compared to the hydrophobic compound 1.

To verify that the release of compound 2 (hsp90 inhibitor) from our star polymer C was pH dependent, drug release was monitored under three different pH ranges: pH = 7.4, 5.5, and 2. We monitored the release of the drug using LC–MS and confirmed its weight by mass spectrometry (Figures 2 and

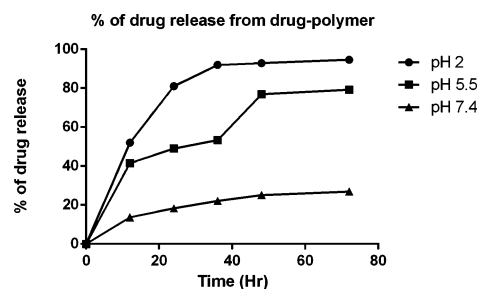


Figure 2. Cumulative release of compound 2 from the 2-loaded polymer (C).

S11A-C, Supporting Information). The data in Figure 2 shows the release of compound 2 over time. At pH 7.4 (corresponding to physiologic pH), 20% of compound 2 was released from the polymer after 24 h, and \sim 25% was released after 72 h. In contrast, at pH 5.5 (corresponding to the pH of an endosome),⁴³ 50% and 80% of compound 2 was released from the polymer at 24 and 72 h, respectively. At pH 2, the release was \sim 95% in 36 h. These data prove that our compound is rapidly released, and they suggest that the maximum release is 80% at pH 5.5, which is typical for endosomal environments.

To verify the cell permeation ability of polymer C particles, a fluorescently tagged molecule was synthesized. Star polymer C was chemically conjugated to fluorescein–isothiocyanate (FITC) to form star polymer D (Scheme 1). We conjugated compound 2, polymer B, and FITC in a 1:100:4 ratio. Using fluorescence microscopy, we investigated the morphology of HCT116 cells treated with media alone, a fluorescent carbocyanine dye (Vybrant Dio dye), or star polymer D. HCT116 cells treated with polymer D emitted light in the 500–550 nm range, which was similar to cells treated with the control dye (Figure 3, compare images 2 and 3). Star polymer

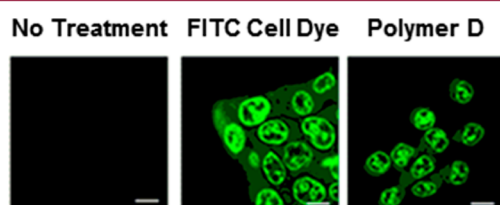


Figure 3. Star polymer D permeates HCT-116 cells. Cells were treated for 24 h with media alone (no treatment; negative control), 25 μM star polymer D, or for 30 min with Vybrant Dio V22886 carbocyanine dye (FITC Cell Dye; 30 nM; positive control). A representative figure is shown for each treatment group, and white bars indicate 10 μm .

D staining was localized to the intracellular space and the nucleus (Figure 3, image 3). These data indicate that star polymer D permeated HCT116 cells and that their localization was diffusely spread throughout the cell and nucleus.

We have previously reported that compound 1 induces caspase 3-dependent apoptosis.²¹ To verify that star polymer C inhibits cell proliferation by the same mechanism, we examined cellular morphology, expression of early/intermediate apoptotic markers, and caspase 3/7 activation in treated cells. Cell rounding and DNA condensation was observed as early as 24 h following treatment with compound 1 (5 μM) or star polymer C (5 μM = 1.16 μM loading of compound 2) (Figure 4A,B, yellow arrows). After 48 h, star polymer C treated cells stained positive for phosphatidylserine (PS)-bound Annexin A5 (or Annexin V; Figure 4C–F). PS is presented on the outer leaflet of the plasma membrane during the early and intermediate stages of apoptosis, and labeled annexin V can be used as a probe for PS due to its high binding affinity for the aminophospholipid.^{44,45}

To determine whether the caspase 3-dependent apoptotic pathway was activated by star polymer C, we used a commercially available kit to measure caspase 3/7 activation in treated cells. After 48 h of treatment, both the hsp90 inhibitor 17-allylamino-17-demethoxygeldanamycin (17-AAG) and compound 1 induce caspase 3/7 activation by 10-fold and 6-fold, respectively, above DMSO-treated cells (Figure 4G). Similar to compound 1, treatment with star polymer C induced caspase 3/7 activation in treated cells by 5-fold above the control or star polymer alone (B). Together these data confirm that star polymer C induces apoptosis through a caspase 3-dependent mechanism, which is the same as the parent compound.

In conclusion, our novel hsp90 inhibitor, compound 1, was successfully conjugated to the star polymer B and was effectively delivered to cells using this nanoparticle (star polymer C). We verified that star polymer C is cytotoxic to a colon cancer cell line, that the manner of drug release from the polymer is pH-dependent, and that localization of the polymers

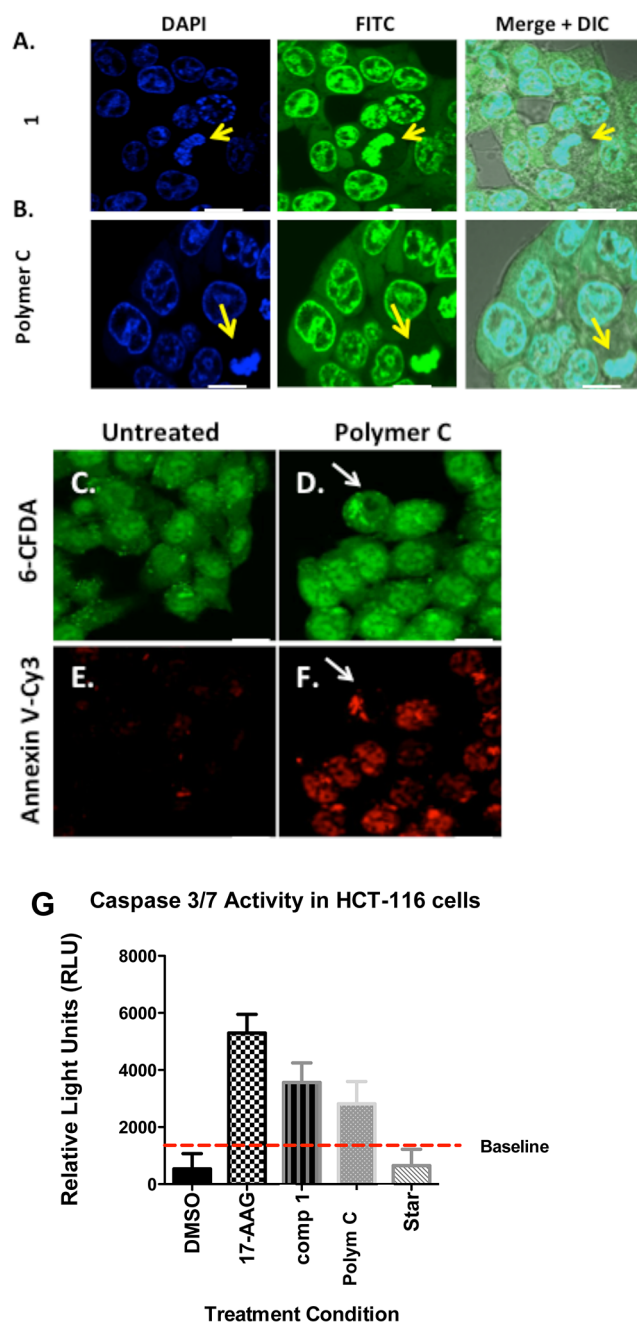


Figure 4. Star polymer C induces apoptosis in HCT-116 cells. (A,B) HCT116 cells were treated (24 h) with compound 1 (5 μM) or star polymer C (5 μM = 1.16 μM of compound 2). Cells are stained for DNA (DAPI) and cell lipids (FITC). Yellow arrows indicate DNA condensation. White bars indicate 10 μm . (C–F) HCT116 cells treated for 48 h with media (C,E) or with star polymer C (D,F). Cells were labeled with 6-carboxyfluorescein diacetate (6-CFDA) to show cell viability (C,D) and with Annexin V-Cy3 (E,F) to indicate apoptotic cells. White arrows point to a cell with a condensed nucleus and Annexin V-positive staining. White bars indicate 10 μm . (G) Caspase 3/7 activity in HCT116 cells treated for 48 h with the hsp90 inhibitor 17-AAG (100 nM), compound 1 (5 μM), star polymer C (5 μM = 1.16 μM of compound 2), or star polymer B (5 μM).

following cell entry is diffuse (using star polymer D). Further, like the parent compound, we showed that star polymer C induces apoptosis by a caspase 3-dependent pathway. Compound 1 is an ideal molecule for advancement into preclinical studies given its unique mechanism of action on

hsp90. These studies have shown that we can deliver this molecule effectively and increase its cytotoxicity over the parent compound. Given that star polymers are nontoxic and stable, they reliably enter cells, they consistently release their drug, and the drug payload is easy to calculate, this system is now ready for testing in small animal models.

■ ASSOCIATED CONTENT

Supporting Information

Experimental details, biological assays, and imaging experiments. This material is available free of charge via the Internet at <http://pubs.acs.org>.

■ AUTHOR INFORMATION

Corresponding Author

*(S.R.M.) E-mail: s.mcalpine@unsw.edu.au. Tel: +61-4-1672-8896.

Funding

We thank the University of New South Wales (UNSW) for support of S.J.K. and D.M.R. as well as NIH 1R01CA137873 for support of this work. C.B. is thankful for his Future Fellowship from ARC.

Notes

The authors declare no competing financial interest.

■ ABBREVIATIONS

FITC, fluorescein–isothiocyanate; GPC, gel permeation chromatography; LC–MS, liquid chromatography–mass spectrometry; UV–vis, ultraviolet–visible spectroscopy; hsp90, heat shock protein 90; GI, growth inhibition; DMSO, dimethylsulfoxide; Pgp, permeability glycol protein

■ REFERENCES

- (1) Bohonowych, J. E.; Gopal, U.; Isaacs, J. S. Hsp90 as a gatekeeper of tumor angiogenesis: clinical promise and potential pitfalls. *J. Oncol.* **2010**, *2010*, 412–485.
- (2) Jolly, C.; Morimoto, R. I. Role of the heat shock protein response and molecular chaperones in oncogenesis and cell death. *J. Natl. Cancer Inst.* **2000**, *92*, 1564–1572.
- (3) Neckers, L.; Ivy, S. P. Heat shock protein 90. *Curr. Opin. Oncol.* **2003**, *15*, 419–424.
- (4) Neckers, L. Hsp90 inhibitors as novel cancer chemotherapeutic agents. *Trends Mol. Med.* **2002**, *8*, S55–S61.
- (5) Parsell, D. A.; Lindquist, S. The function of heat-shock proteins in stress tolerance: degradation and reactivation of damaged proteins. *Annu. Rev. Genet.* **1993**, *27*, 437–496.
- (6) Parsell, D. A.; Taulien, J.; Lindquist, S. The role of heat-shock proteins in thermotolerance. *Philos. Trans. R. Soc. London, Ser. B* **1993**, *339*, 279–285 discussion, 285–286.
- (7) Chiosis, G.; JHuezo, H.; Rosen, N.; Mimgaugh, E.; Whitesell, L.; Neckers, L. 17AAG: low target binding affinity and potent cell activity—finding an explanation. *Mol. Cancer Ther.* **2003**, *2*, 123–129.
- (8) Neckers, L. Heat shock protein 90: the cancer chaperone. *J. Biosci.* **2007**, *32*, 517–530.
- (9) Takayama, S.; Reed, J. C.; Homma, S. Heat-shock proteins as regulators of apoptosis. *Oncogene* **2003**, *22*, 9041–9047.
- (10) Kamal, A.; Thao, L.; Sensintaffar, J.; Zhang, L.; Boehm, M. F.; Fritz, L. C.; Burrows, F. J. A high-affinity conformation of Hsp90 confers tumour selectivity on Hsp90 inhibitors. *Nature* **2003**, *425*, 407–410.
- (11) Clinical Trials. <http://www.clinicaltrials.gov>.
- (12) Neckers, L.; Workman, P. Hsp90 molecular chaperone inhibitors: Are we there yet? *Clin. Cancer Res.* **2012**, *18*, 64–76.

- (13) Trepel, J.; Mollapour, M.; Giaccone, G.; Neckers, L. Targeting the dynamic HSP90 complex in cancer. *Nat. Rev. Cancer* **2010**, *10*, 537–549.

- (14) Beliakoff, J.; Whitesell, L. Hsp90: An emerging target for breast cancer therapy. *Anticancer Drugs* **2004**, *15*, 651–662.

- (15) Workman, P. Altered states: Selectively drugging the Hsp90 cancer chaperone. *Trends Mol. Med.* **2004**, *10*, 47–51.

- (16) Carroll, C. L.; Johnston, J. V. C.; Kekec, A.; Brown, J. D.; Parry, E.; Cajica, J.; Medina, I.; Cook, K. M.; Corral, R.; Pan, P.-S.; McAlpine, S. R. Synthesis and Cytotoxicity of Novel Sansalvamide A Derivatives. *Org. Lett.* **2005**, *7*, 3481–3484.

- (17) Otrubova, K.; Lushington, G. H.; Vander Velde, D.; McGuire, K. L.; McAlpine, S. R. A comprehensive study of Sansalvamide A derivatives and their structure–activity relationships against drug-resistant colon cancer cell lines. *J. Med. Chem.* **2008**, *51*, 530–544.

- (18) Pan, P. S.; Vasko, R. C.; Lopera, S. A.; Johnson, V. A.; Sellers, R. P.; Lin, C.-C.; Pan, C.-M.; Davis, M. R.; Ardi, V. C.; McAlpine, S. R. A comprehensive study of Sansalvamide A derivatives: their structure–activity relationships and their binding mode to Hsp90. *Bioorg. Med. Chem.* **2009**, *17*, 5806–5825.

- (19) Vasko, R. C.; Rodriguez, R. A.; Cunningham, C. N.; Ardi, V. C.; Agard, D. A.; McAlpine, S. R. Mechanistic studies of Sansalvamide A-Amide: an allosteric modulator of Hsp90. *ACS Med. Chem. Lett.* **2010**, *1*, 4–8.

- (20) Alexander, L. D.; Partridge, J. R.; Agard, D. A.; McAlpine, S. R. A small molecule that preferentially binds the closed Hsp90 conformation. *Bioorg. Med. Chem. Lett.* **2011**, *21*, 7068–7071.

- (21) Ardi, V. C.; Alexander, L. D.; Johnson, V. A.; McAlpine, S. R. Macrocycles that inhibit the binding between heat shock protein 90 and TPR-containing proteins. *ACS Chem. Biol.* **2011**, *6*, 1357.

- (22) Kunicki, J. B.; Petersen, M. N.; Alexander, L. D.; Ardi, V. C.; McConnell, J. R.; McAlpine, S. R. Synthesis and evaluation of biotinylated Sansalvamide A analogs and their modulation of Hsp90. *Bioorg. Med. Chem. Lett.* **2011**, *21*, 4716–4719.

- (23) Davis, M. R.; Singh, E. K.; Wahyudi, H.; Alexander, L. D.; Kunicki, J.; Nazarova, L. A.; Fairweather, K. A.; Giltrap, A. M.; Jolliffe, K. A.; McAlpine, S. R. Synthesis of Sansalvamide A peptidomimetics: triazole, oxazole, thiazole, and pseudoproline containing compounds. *Tetrahedron* **2012**, *68*, 1029–1051.

- (24) Ramsey, D. M.; McConnell, J. R.; Alexander, L. D.; Tanaka, K. W.; Vera, C. M.; McAlpine, S. R. A new Hsp90 inhibitor that exhibits a novel biological profile. *Bioorg. Med. Chem. Lett.* **2012**, *22*, 3287–3290.

- (25) Sellers, R. P.; Alexander, L. D.; Johnson, V. A.; Lin, C.-C.; Savage, J.; Corral, R.; Moss, J.; Slugocki, T. S.; Singh, E. K.; Davis, M. R.; Ravula, S.; Spicer, J. E.; Oelrich, J. L.; Thornquist, A.; Pan, C.-M.; McAlpine, S. R. A third generation of Sansalvamide A derivatives: Design and synthesis of Hsp90 Inhibitors. *Bioorg. Med. Chem.* **2010**, *18*, 6822–6856.

- (26) Wang, Y.; Grayson, S. M. Approaches for the preparation of non-linear amphiphilic polymers and their applications to drug delivery. *Adv. Drug Delivery Rev.* **2012**, *64*, 852–865.

- (27) Duan, S.; Cai, S.; Xie, Y.; Bagby, T. R.; Forrest, M. L. Synthesis and characterization of a multiarm poly(acrylic acid) star polymer for application in sustained delivery of cisplatin and a nitric oxide prodrug. *J. Polym. Sci., Part A: Polym. Chem.* **2012**, *50*, 2715–2724.

- (28) Lovell, J. F.; Huynh, E.; Macdonald, T. D.; Lin, Q.; Zheng, G. Biodegradable star polymers shine for cancer drug delivery. *Nanomedicine* **2011**, *6*, 1155.

- (29) Sulistio, A.; Lowenthal, J.; Blencowe, A.; Bongiovanni, M. N.; Ong, L.; Gras, S. L.; Zhang, X.; Qiao, G. G. Folic acid conjugated amino acid-based star polymers for active targeting of cancer cells. *Biomacromolecules* **2011**, *12*, 3469–3477.

- (30) Alconcel, S. N. S.; Baas, A. S.; Maynard, H. D. FDA-approved poly(ethylene glycol)-protein conjugate drugs. *Polym. Chem.* **2011**, *2*, 1442–1448.

- (31) Boyer, C.; Davis, T. P. One-pot synthesis and biofunctionalization of glycopolymers via RAFT polymerization and thiol–ene reactions. *Chem. Commun.* **2009**, 6029–6031.

(32) Boyer, C.; Bulmus, V.; Liu, J. Q.; Davis, T. P.; Stenzel, M. H.; Barner-Kowollik, C. Well-defined protein–polymer conjugates via in situ RAFT polymerization. *J. Am. Chem. Soc.* **2007**, *129*, 7145–7154.

(33) Boyer, C.; Liu, J.; Bulmus, V.; Davis, T. P.; Barner-Kowollik, C.; Stenzel, M. H. Direct synthesis of well-defined heterotelechelic polymers for bioconjugations. *Macromolecules* **2008**, *41*, 5641–5650.

(34) Liu, J.; Duong, H.; Whittaker, M. R.; Davis, T. P.; Boyer, C. Synthesis of functional core, star polymers via RAFT polymerization for drug delivery applications. *Macromol. Rapid Commun.* **2012**, *33*, 760–767.

(35) Zastre, J.; Jackson, J.; Bajwa, M.; Liggins, R.; Iqbal, F.; Burt, H. Enhanced cellular accumulation of a P-glycoprotein substrate, rhodamine-123, by caco-2 cells using low molecular weight methoxypolyethylene glycol-block-polycaprolactone diblock copolymers. *Eur. J. Pharm Biopharm.* **2002**, *54*, 299–309.

(36) Schroeder, A.; Heller, D. A.; Winslow, M. M.; Dahlman, J. E.; Pratt, G. W.; Langer, R.; Jacks, T.; Anderson, D. G. *Nat. Rev. Cancer* **2012**, *12*, 39–45.

(37) Banerjee, I.; Pangule, R. C.; Kane, R. S. Antifouling coatings: recent developments in the design of surfaces that prevent fouling by proteins, bacteria, and marine organisms. *Adv. Mater.* **2011**, *23*, 690–718.

(38) Gabizon, A. A. Stealth liposomes and tumor targeting: one step further in the quest for the magic bullet. *Clin. Cancer Res.* **2001**, *7*, 223–225.

(39) Bjugstad, K. B.; Redmond, D. E., Jr.; Lampe, K. J.; Kern, D. S.; Sladek, J. R., Jr.; Mahoney, M. J. Biocompatibility of PEG-based hydrogels in primate brain. *Cell Transplant.* **2008**, *17*, 409–415.

(40) Jackson, A. W.; Stakes, C.; Fulton, D. A. The formation of core cross-linked star polymer and nanogel assemblies facilitated by the formation of dynamic covalent imine bonds. *Polym. Chem.* **2011**, *2*, 2500–2511.

(41) Jackson, A. W.; Fulton, D. A. The formation of core cross-linked star polymers containing cores cross-linked by dynamic covalent imine bonds. *Chem. Commun.* **2010**, *46*, 6051–6053.

(42) Rodriguez, R. A.; Pan, P.-S.; Pan, C.-M.; Ravula, S.; Lapera, S. A.; Singh, E. K.; Styers, T. J.; Brown, J. D.; Cajica, J.; Parry, E.; Otrubova, K.; McAlpine, S. R. Synthesis of second generation Sansalvamide A derivatives: novel templates as potent anti-tumor agents. *J. Org. Chem.* **2007**, *72*, 1980–2002.

(43) Kneipp, J.; Kneipp, H.; Wittig, B.; Kneipp, K. Following the dynamics of pH in endosomes of live cells with SERS nanosensors. *J. Phys. Chem. C* **2010**, *114*, 7421–7426.

(44) Blankenberg, F. G.; Naumovski, L.; Tait, J. F.; Post, A. M.; Strauss, H. W. Imaging cyclophosphamide-induced intramedullary apoptosis in rats using ^{99m}Tc-radiolabeled annexin V. *J. Nucl. Med.* **2001**, *42*, 309–316.

(45) Martin, S. J.; Reutelingsperger, C. P. M.; McGahon, A. J. Early redistribution of plasma membrane phosphatidylserine is a general feature of apoptosis regardless of the initiating stimulus: inhibition by overexpression of Bcl-2. *J. Exp. Med.* **1995**, *182*, 1545–1556.